CHAPTER 6: Comparative Study of Perovskite and Ruddlesden Popper (RP) for Lead (Pb) and Lead-free Halides

6.1 Introduction

In the fifth chapter, it is discussed that the $CsPbBr_3$ bulk sample synthesized by the cold sintering method was found to be structurally and thermally stable at room temperature. It also discusses the I-V hysteresis of the bulk $CsPbBr_3$ sample with continuous exposure to AM 1.5 G Sun light for 3 h. Similarly, IV hysteresis for lead and lead-free halide materials is studied in detail in the present chapter. Therefore, the conduction mechanism [forward scan (FS) as well as reverse scan (RS)] has been studied with continuous exposure to AM 1.5 G Sunlight for 3 h. All compounds ($CsPbBr_3$, $CsSnBr_3$, Cs_2PbBr_4, and Cs_2SnBr_4) were synthesized by cold sintering method via solid-state reaction route at room temperature. In the present chapter, the comparative study of perovskite and Rudlesden-Popper (RP) materials has been discussed.

6.2 Experimental Procedure

All compounds ($CsPbBr_3$, $CsSnBr_3$, Cs_2PbBr_4, and Cs_2SnBr_4) were prepared by Cold sintering (CS)–Solid-state reaction (SSR) route. To synthesize these samples, CsBr (99.999%, Aldrich), CsBr (99.9%, Alfa Aesar), $SnBr_2$ (99.2%, Alfa Aesar), and $PbBr_2$ (98%, Aldrich) powders have been weighed in stoichiometric quantities. The synthesis process and all experimental details have already been discussed in the third and fourth chapters, respectively.

6.3 Results and Discussion

6.3.1 Structural Studies

XRD patterns of $CsPbBr_3$ and $CsSnBr_3$ materials along with their Rudlesden Popper have been recorded at room temperature with step size 0.1 in the 2θ range from 5 to 70˚ and shown in Fig. 6.1(a,b), respectively. It is observed that all four samples show orthorhombic structure at room temperature.

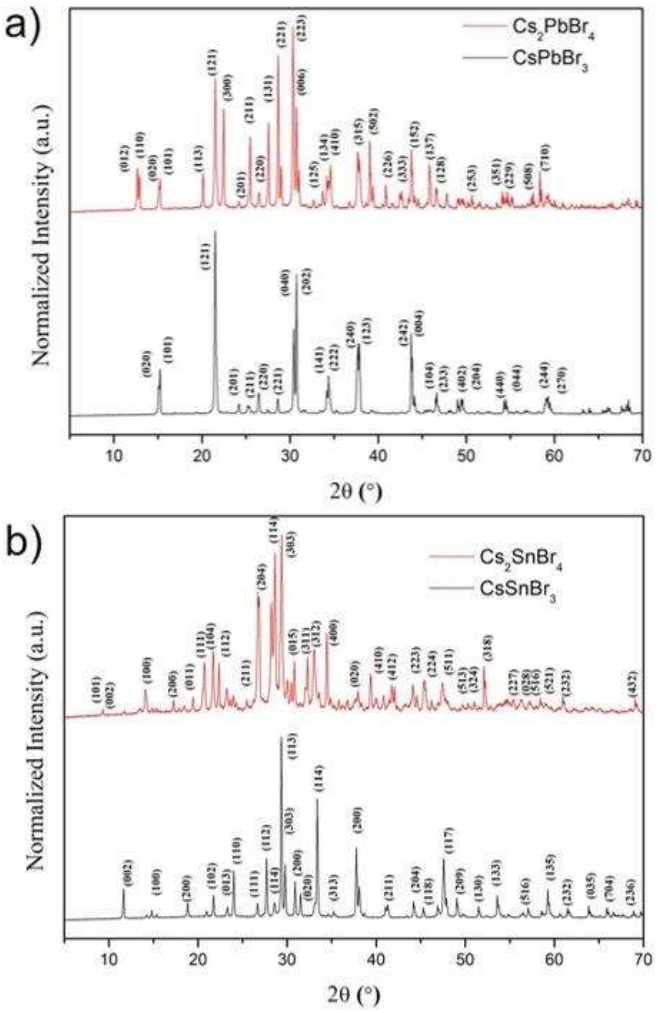

Figure 6.1: (a and b) represents the XRD patterns for $CsPbBr_3$, $CsSnBr_3$, Cs_2PbBr_4, and Cs_2SnBr_4, respectively.

6.3.2 Current-Voltage Hysteresis Studies

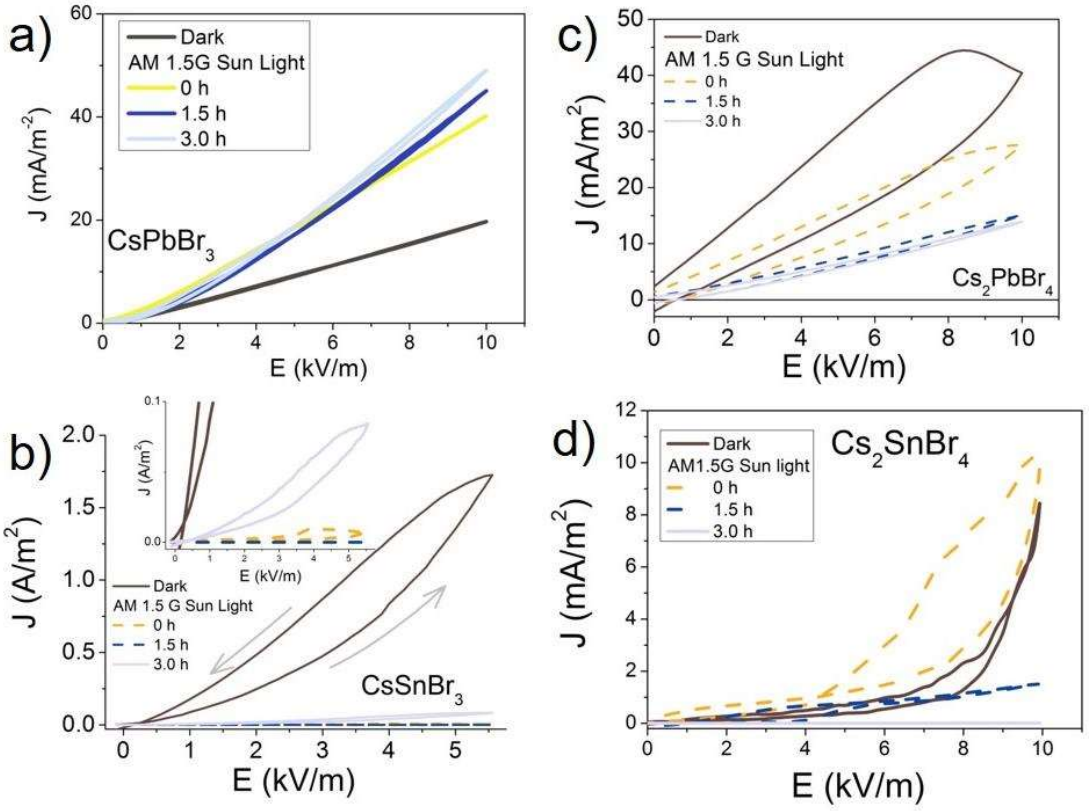

Figure 6.2: Observation of current density with electric field in perovskite ($CsPbBr_3$ and $CsSnBr_3$) and Ruddlesden-Popper(Cs_2PbBr_4 and Cs_2SnBr_4)materials with an illumination of AM 1.5 G Sunlight.

Fig. 6.2 shows the current-voltage hysteresis for perovskite ($CsPbBr_3$ and $CsSnBr_3$) and Rudlesden–Popper materials (Cs_2PbBr_4 and Cs_2SnBr_4) exposed to AM 1.5 G sunlight at different time intervals of 1.5 h. Forward scanning (FS) and reverse scanning (RS) have been done to understand the I-V hysteresis of these materials. Current and voltage have been replaced by current density (J) and electric field (E), respectively. The surface area A = 100 mm^2 and the distance between the electrodes d = 1 mm are used. Fig. 6.2(a, b, c, d) AM represents the current density variation with electric field in continuous illumination of 1.5G of sunlight. In this chapter, a comparative study of perovskite and Rudlesden-Popper is done

in the same way as in the previous chapter 5. It is observed that the cesium lead bromide ($CsPbBr_3$) perovskite sample shows minimum hysteresis as compared to other synthesized materials, as shown in Fig. 6.2(a). However, it is observed that lead-based materials have minimum hysteresis as compared to lead-free halide materials. Exposure to AM 1.5G sunlight resulted in faster degradation of lead-free samples than lead-based halides.

To understand this behavior, the FS and RS curves are fitted with $J=KE^n$ Perovskite and Ruddelesden-Popper materials. The FS and RS are fitted easily for lead-based materials as compared to the lead-free materials (see Fig. 6.3(a,b)) but lead-free halides could not be fitted very well because of the more degradation in the exposure of AM 1.5G sunlight (see Fig. 6.4(a,b)).

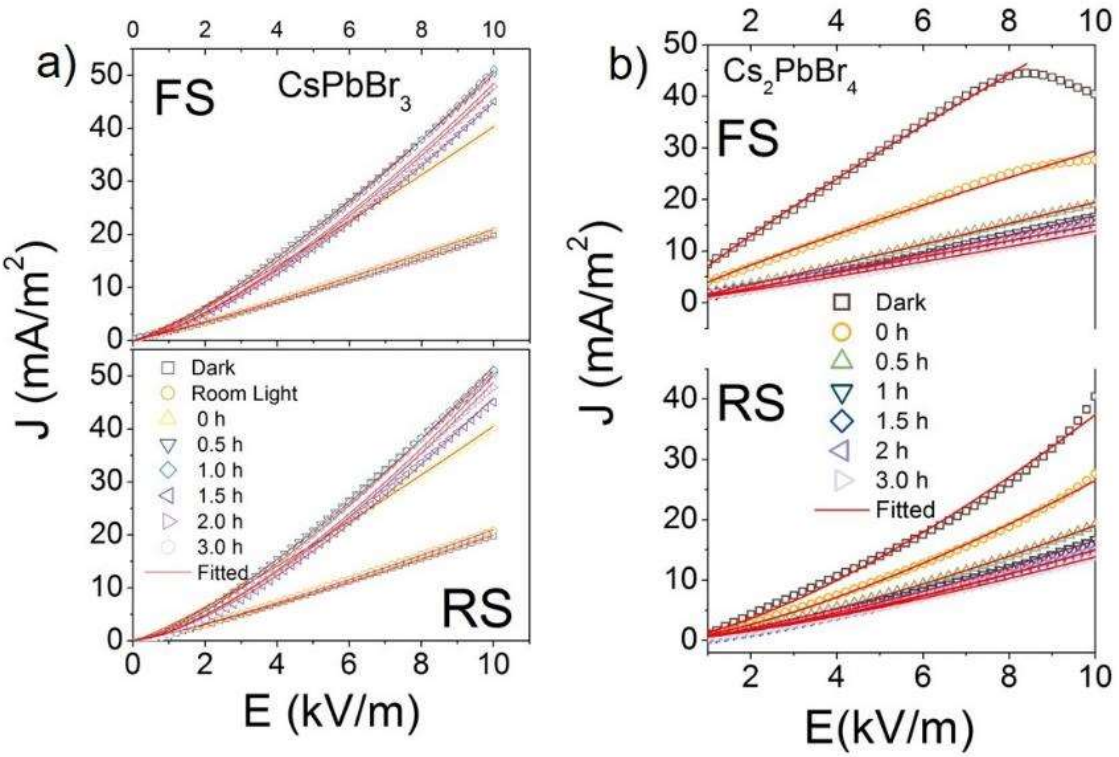

Figure 6.3: FS and RSfitted from $J=KE^n$for $CsPbBr_3$ and Cs_2PbBr_4in dark light and with the illumination of AM 1.5 G Sunlight (at a few intervals of time, 0h, 0.5h, 1h, 1.5h, 2h, 2.5h, 3.0h).

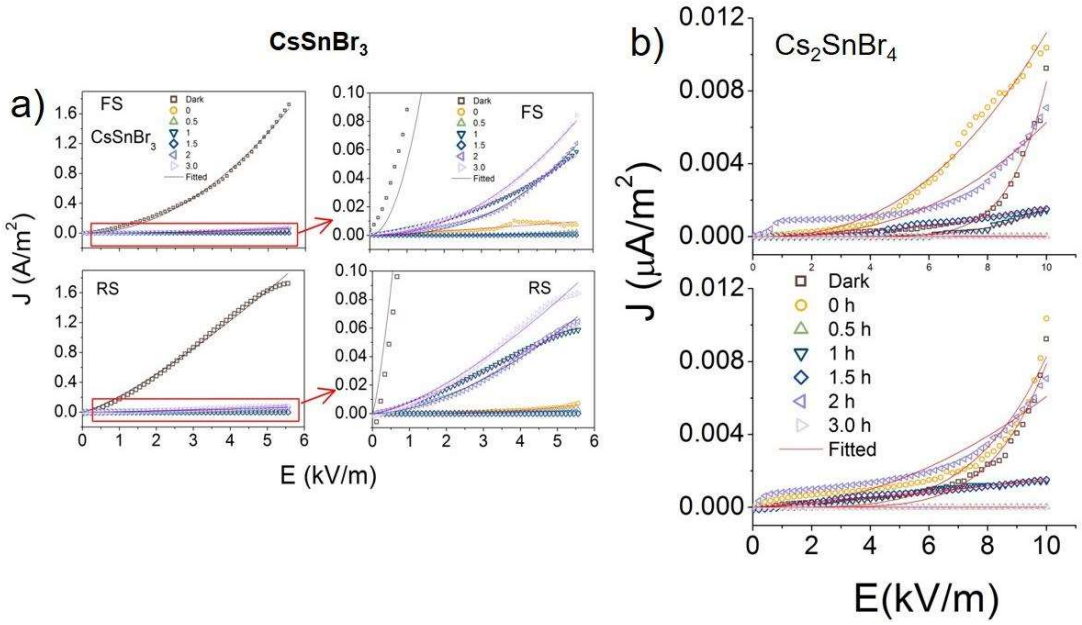

Figure 6.4: FS and RS fitted from $J=KE^n$ for $CsSnBr_3$ (zoomed images of current density on the right side of Fig. a) and Cs_2SnBr_4 in dark light and with the illumination of AM 1.5 G Sunlight (at a few intervals of time, 0h, 0.5h, 1h, 1.5h, 2h, 2.5h, 3.0h).

The conductivity variation (σ-E curves) of the samples has been plotted for FS and RS. The conductivity with electric field relation details has been discussed in previous chapter 5. The difference in the behavior of FS and RS is observed, as shown in Fig. (6.5 and 6.6). It is observed that the conductivity decreases to ~1.5 kV/m in the FS of Cs_2PbBr_4. After that, it stabilizes (1.5 kV/m < E < 8 kV/m) and then slows down (E > 8 kV/m) when AM is exposed to 1.5G sunlight (see Fig. 6.5(b)).Whereas in the RS of Cs_2PbBr_4, the conductivity rapidly increases to ~2 kV/m and it gradually increases to (2 kV/m < E < 8 kV/m), then it rapidly increases to (E > 8 kV/m) increases. The conductivity of the $CsSnBr_3$ material increases sharply in the range of electric field (~E > 1 kV/m) for both FS and RS.While the conductivity in the Cs_2SnBr_4 sample gradually decreases (up to ~1.5 kV/m) then it stabilizes (up to 1.5 kV/m < E < 8 kV/m). After that, it increases faster (E > 8 kV/m). It is observed that the conductivity of the cesium tin bromide ($CsSnBr_3$) sample is higher than that of other synthesized materials,

but the loss of this material decreases faster than other samples when exposed to AM 1.5 G sunlight.

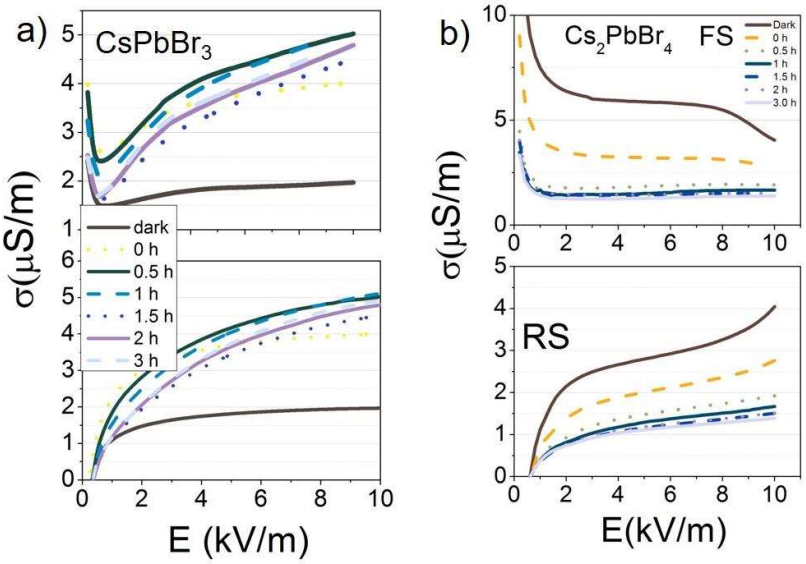

Figure 6.5: Variation of (σ-E)for $CsPbBr_3$ and Cs_2PbBr_4in dark light and with the illumination of AM 1.5 G Sunlight (at a few intervals of time, 0h, 0.5h, 1h, 1.5h, 2h, 2.5h, 3.0h).

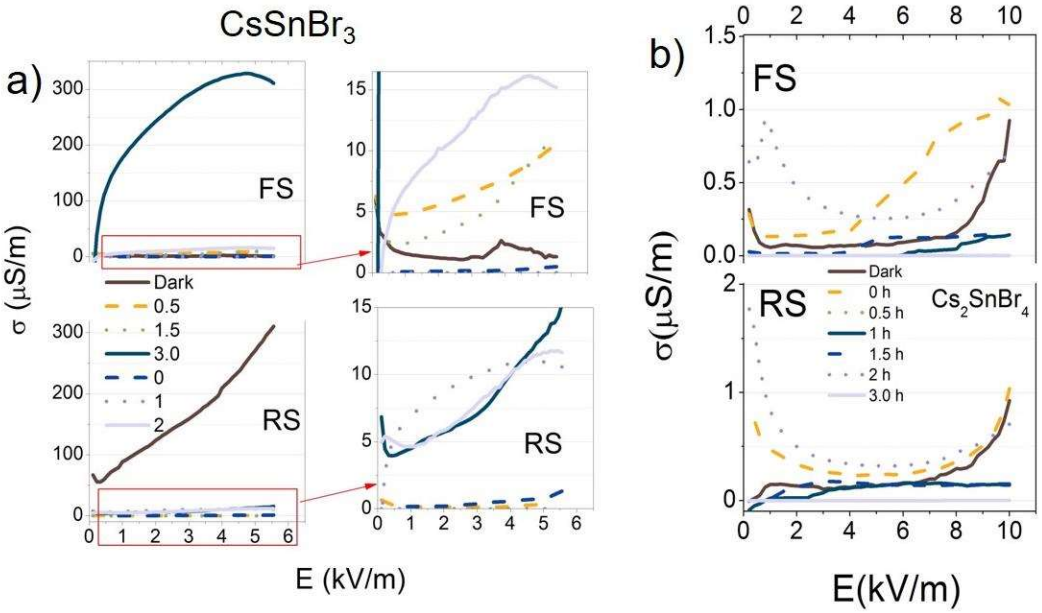

Figure 6.6: Variation of (σ-E) for $CsSnBr_3$(zoomed images of conductivity are indicated by the arrow sign on the right side of Fig. a) and Cs_2SnBr_4 in dark light and with the illumination of AM 1.5 G Sunlight (at a few intervals of time, 0h, 0.5h, 1h, 1.5h, 2h, 2.5h, 3.0h).

It is difficult to see the conductivity behavior of the sample only by the σ-E curves. Therefore, the comparative conduction behavior can be understood as a deviation from the Drude relation ($\sigma=\sigma_p+\sigma_0 e^{(k_1 q\beta d) E_0}$) and fit the σ-E curves with the modified Arrhenius relation. As we have discussed the RP material above, more degradation is observed when exposed to AM 1.5 G Sunlight. Therefore, the photoconductivity (just illuminated) and dark conductivity are fitted for the $CsPbBr_3$ and $CsSnBr_3$ samples. It is observed that cesium lead bromide is fitted much better than cesium tin bromide due to the minimum hysteresis for FS and RS (see Fig. 6.7(a,b)). Furthermore, the $CsSnBr_3$ sample shows maximum hysteresis when exposed to AM 1.5 G Sunlight (just illuminated), as shown in Fig. 6.7(b).

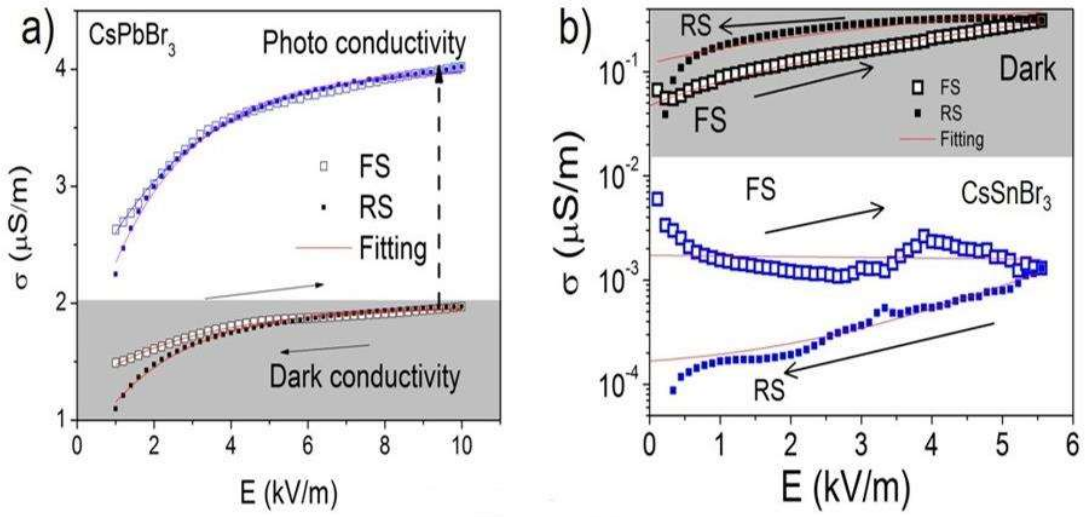

Figure 6.7: Variation of photoconductivity (just illuminated) and dark conductivityfor $CsPbBr_3$ and $CsSnBr_3$ samples.

The variation of the extracted parameter 'n' can be understood with n-time (h) curves, as depicted in Fig. 6.8. It is observed that the value of 'n' varies with the illumination. In this chapter, a comparative study has been made to understand the current-voltage hysteresis. The value of 'n' varies from 1.1 to 1.5 for the Cs_2PbBr_3 sample in FS and RS. Further, the 'n' value

is increased to 90 min and then stabilized. Ideally, the value of 'n' is equal to 1 for the ohmic behavior of the material. But here for cesium lead bromide ($CsPbBr_3$) the value of 'n' is more than 1 (1.1 to 1.5) due to the trap-filled state. Whereas in RP material (Cs_2PbBr_4), in FS the value of 'n' is increased for 60 min and then stabilized (see Fig. 6.8(c)). It is found that the value of 'n' in FS is almost equal to 1 indicating ohmic behavior but in RS at n~1.4 it shows a trap-filled state and becomes stable. Furthermore, the lead-free perovskite and RP material show different conduction behavior and further degradation when exposed to AM 1.5 G sunlight. It is observed that the value of 'n' shows disorder behavior up to 90 min and stabilizes after 90 min in FS and RS for $CsSnBr_3$ and Cs_2SnBr_4 materials when AM 1.5 G Sunlight is exposed, as shown in Fig. 6.8(b,d). The 'n' value in RS for the $CsSnBr_3$ sample is about 1.5 due to the trap-filled state. Whereas 'n' is equal to 2 in FS which denotes a trap-free state. But in the case of the Cs_2SnBr_4 sample, the value of 'n' in FS and RS is equal to 2 due to trap free state.

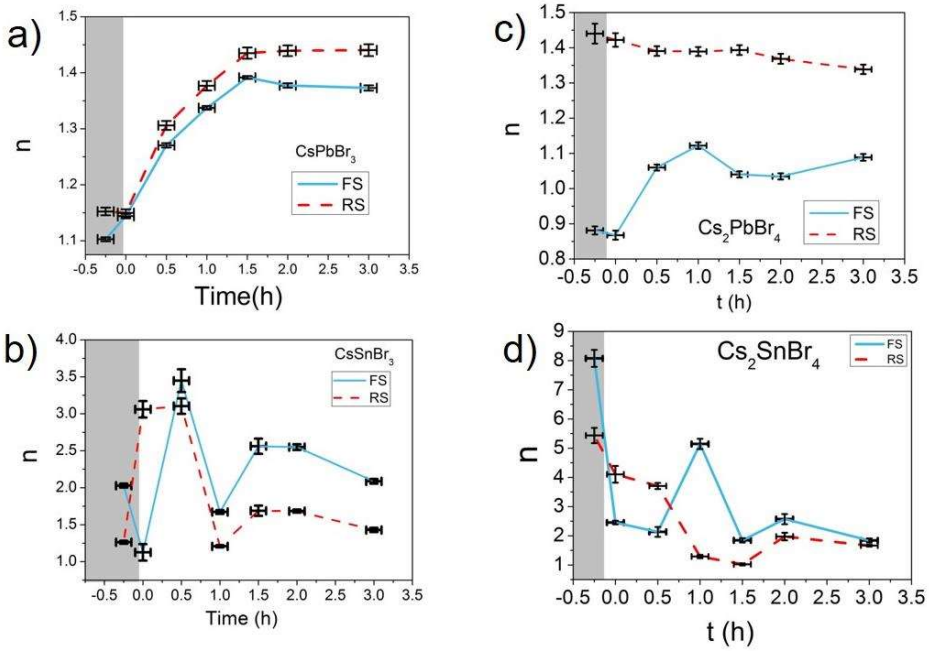

Figure 6.8: Variation of extracted parameter 'n' from fitting $J=KE^n$ for FS and RS.

Furthermore, the time-dependent variation of discharge current with bias voltage has been studied to understand the mechanism of photoconduction for all samples. It is observed that the cesium lead bromide ($CsPbBr_3$) sample has a positive photoresponse current with time when a voltage is applied.

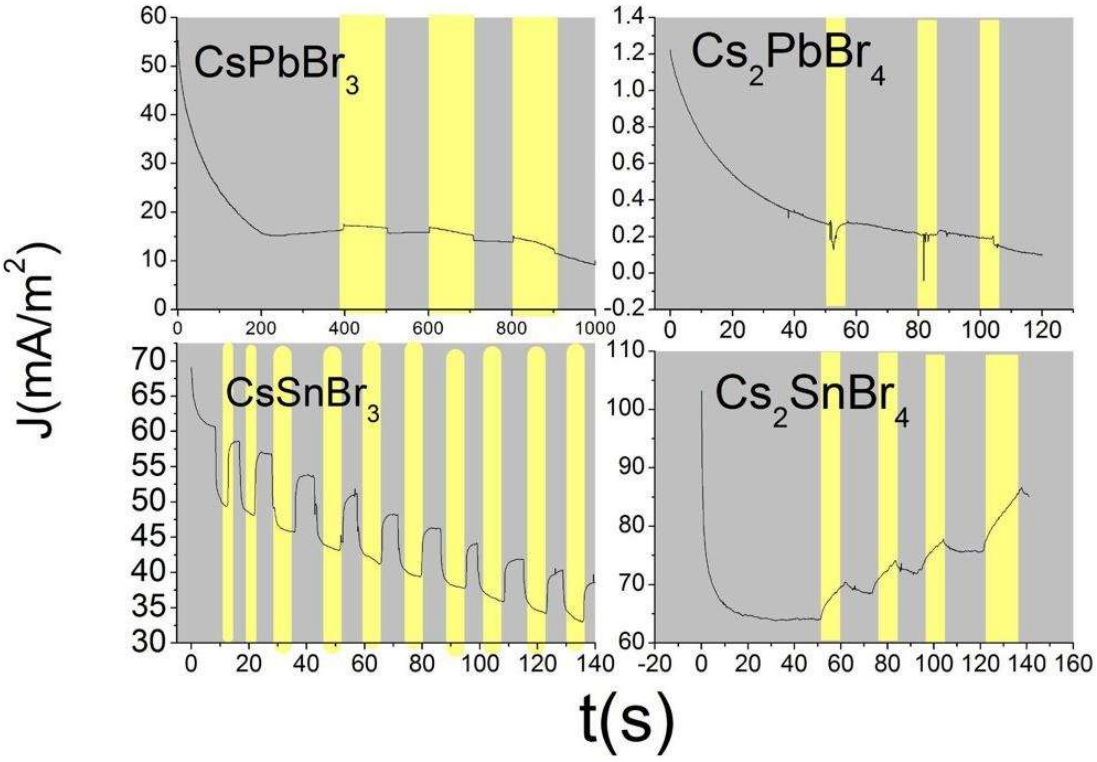

Figure 6.9: Photoresponse current vs time with the bias electric field.

But the other three samples (Cs_2PbBr_4, $CsSnBr_3$, and Cs_2SnBr_4) have a negative photoresponse current with time when voltage is applied (Fig. 6.9). In addition, it is also observed that the $CsSnBr_3$ material has the maximum photoresponse current over time among all the materials, due to which its conductivity is higher than that of other synthesized samples.

6.3.3 Optical Properties

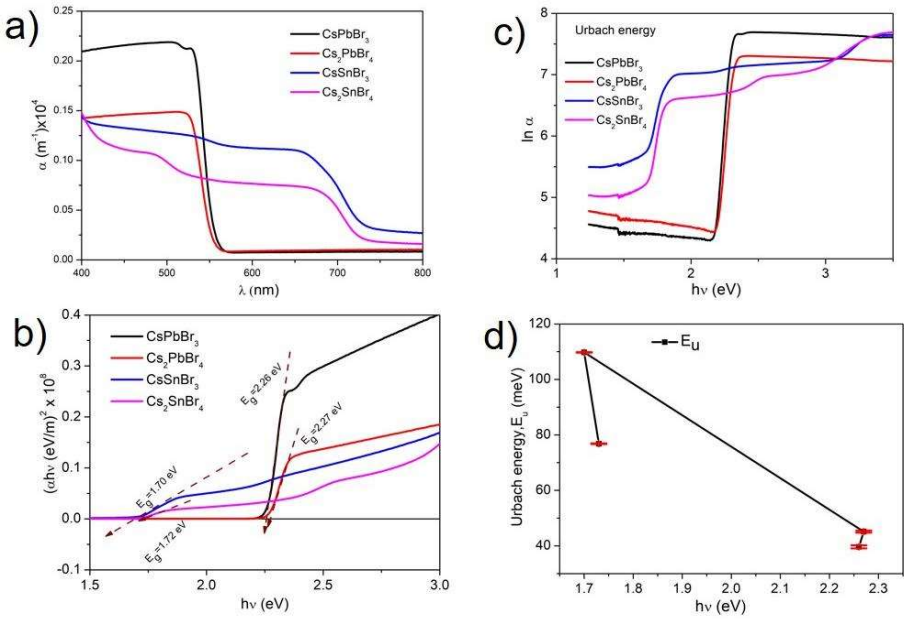

Figure 6.10: Optical absorption spectra for $CsPbBr_3$, Cs_2PbBr_4, CsSnBr3, and Cs_2SnBr_4 samples (b) direct band gap energy calculation from Tauc relation (c) Plot of ln (α) versus *hν* (eV) for Urbach energy (E_u) (d) Variation of *hν* (eV) verses Urbach energy (E_u).

The optical spectrum in the wavelength region between 400 nm and 800 nm is examined by an ultraviolet-visible (UV) spectrometer. A strong absorption edge is found at ~555 nm for both $CsPbBr_3$ and Cs_2PbBr_4 samples. Whereas, the absorption edges are obtained at ~725 nm for both $CsSnBr_3$ and Cs_2SnBr_4 samples. Further, the value of the bandgap energy of the studied samples has been estimated. Therefore, the variance of $(\alpha h\nu)^2$ versus $h\nu$ is plotted (Figure 6.10(b)). The bandgap energy for the material has been estimated by intercepting it with the energy axis. The direct bandgap is estimated to be 1.70 eV ($CsSnBr_3$), 1.72 eV ($CsSnBr_3$), respectively. Whereas in case of $CsPbBr_3$ and Cs_2PbBr_4 it is 2.26 eV and 2.27eV respectively. It can be concluded that Sn-based material has less optical bandgap than 'Pb'

based material and the change in bandgap can be attributed to the smaller ionic radius of Sn^{2+} as compared to the ionic radius of Pb^{2+} [117],[187].

The power factor (p) is calculated to examine the type of the bandgap using the well-known relation [188].

$$(\alpha h\nu) = A\,(h\nu - E_g)^p \tag{6.1}$$

Where E_g, α, $h\nu$, A and p are the optical band gap energy, absorption coefficient, incident photon energy, energy independent constant, is the incident photon energy, and power factor of transition modes, respectively. Taking logarithms of both sides of the equation (6.1), the equation becomes

$$\ln(\alpha h\nu) = p \ln(h\nu - E_g) + \ln A \tag{6.2}$$

Then, compare the equation to the straight-line equation y = mx + c. The slope value (m = p) has been recorded to find the transition mode (p). The plot of ln ($\alpha h\nu$) versus ln ($h\nu$-E_g) has been obtained to verify the power factor (p) for the direct allowed (p = 1/2), direct prohibited (p = 3/2), indirect allowed (p = 2), and indirect prohibited (p = 3) transitions. Hence the value of power factor (p) has been found after the analysis of linear curve fitting. It is observed that in all samples there is a direct allowed transition with a value of 'p' close to 0.5. An exponential portion of the near band edges in optical absorption spectra is called the Urbach tail. An exponential dependence of the absorption coefficient (α) on the photon energy (hν) in the energy range $E<E_g$ is expressed as [189].

$$\alpha = \alpha_0 \exp(h\nu/E_u) \tag{6.3}$$

where E_u and α_o are the Urbach energy, and constant, respectively. Taking the logarithm of both the sides of the above equation (6.3).

$$\ln\alpha = (h\nu/E_u) + \ln \alpha_o \quad (6.4)$$

The Urbach energy has been calculated to plot between the *ln (α)* versus *hν* (eV), as shown in Fig. 6.10(c). Therefore, a linear fit analysis of these curves is performed to estimate the value of Urbach energy (Eu). The value of E_u for 'Pb' based material is around 40-50 meV. In the case of $CsSnBr_3$ and Cs_2SnBr_4 samples, the Urbach energy is ~105 meV and ~80 meV, respectively. It is observed that the value of Urbach Energy (E_u) is higher for Sn-based material than for 'Pb' based material (Fig. 6.10(d)). This can be attributed to more disorder in the structure of the 'Sn' samples as compared to the 'Pb' samples.

6.4 Conclusion

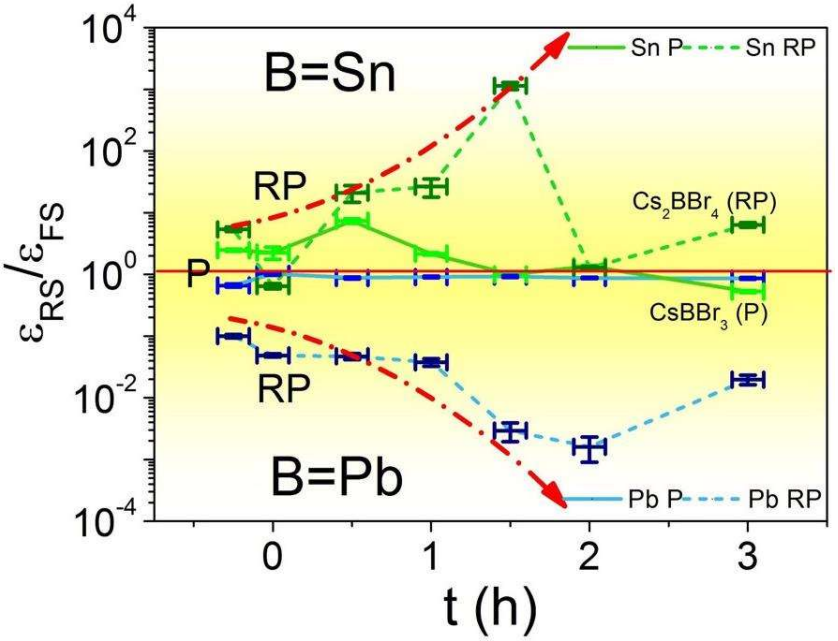

Figure 6.11: Represents the ratio of $\varepsilon_{RS}/\varepsilon_{FS}$ with time in the continuous exposure of AM 1.5 G Sunlight.

All compounds ($CsPbBr_3$, $CsSnBr_3$, Cs_2PbBr_4, and Cs_2SnBr_4) were prepared by Cold sintering (CS)–Solid-state reaction (SSR) route. It is observed that the polarization is higher in RS than FS in 'Sn' samples irrespective of the structure. But polarization is higher in FS than in 'Pb' samples irrespective of the structure. It can be concluded that the 'Pb' based sample has an order of 1000 difference in polarization as compared to the Sn-based samples. It is also observed that the polarization of cesium lead bromide ($CsPbBr_3$) material is in the range of 10^0, due to which it has minimum I-V hysteresis.